Available online at www.sciencedirect.com
ScienceDirect
Engineering Structures 29 (2007) 195–212
ENGINEERING STRUCTURES
www.elsevier.com/locate/engstruct

Cross-sectional properties of complex composite beams

Airil Y. Mohd Yassin[a], David A. Nethercot[b,*]

[a] Faculty of Civil Engineering, Universiti Teknologi Malaysia Johor Bahru, Malaysia
[b] Department of Civil and Environmental Engineering, Imperial College, London, United Kingdom

Received 22 September 2005; received in revised form 15 March 2006; accepted 25 April 2006
Available online 30 June 2006

Abstract

A procedure is presented for the calculation of the key cross-sectional properties of steel–concrete composite beams of complex cross-section. The novel feature of the procedure is the use of functions to describe the shape of the different elements in a cross-section; this permits determination of the cross-sectional properties through appropriate integrations. The formulation is developed in a format that is directly suitable for computer programming, i.e. in matrix forms and operations. It is completely general in terms of the shape of the cross-section. The procedure is applied to a new type of composite beam known as the PCFC (pre-cast cold-formed composite) beam, details of which are explained herein. This is shown to perform better than equivalent, more conventional composite beams at the ultimate condition, but is slightly less efficient when considering some serviceability aspects.

Keywords: Beams; Composite construction; Flexure; Section properties; Structural design

1. Introduction

The earliest known form of steel–concrete composite beam, dating from the late 1800s, comprised a steel beam encased in concrete, as shown in Fig. 1(a). The arrangement was first used in a bridge in Iowa and a building in Pittsburgh [10]. The encasement provides fire protection but also enhances the bending strength of the steel beam. Since ultimate strength design was not known at the time, the basis was an elastic assessment. However, with the introduction of ultimate strength design, the eccentricity between the resultant force in the concrete and that in the steel was recognized as the key factor in determining the effectiveness of the composite action. Intuitively, a steel beam located beneath the concrete element would result in greater eccentricity and would thus perform better than the encased section. Such a configuration is shown in Fig. 1(b) in the form of a steel beam connected to the concrete slab by means of shear connectors [3]. As a way of further increasing the lever arm, the steel beam can be made asymmetric about its major axis, either by increasing the depth or the width (or both) of the lower flange, as shown in Fig. 1(c) and (d) [2]. Moreover, a reinforced concrete beam, shown as Fig. 1(e), can also be loosely regarded as a composite beam but excluded if the definition requires that the steel element should have substantial flexural stiffness when acting alone, something that the rebar clearly does not possess.

The availability of thin cold-formed steel components in the construction industry has led to a new composite configuration, consisting of a steel beam and a composite slab, as shown in Fig. 1(f) [4]. New considerations arise for such a configuration as the slab is no longer solid but profiled, thereby influencing the location of the point of action of the concrete resultant force, the total steel resultant forces (as now there are two sources: the steel beam and the profiled sheeting) and the behaviour of the shear connection. Recently, other new slab systems have also been introduced into composite design such as hollow-cored slabs [6] and pre-cast slabs with a concrete topping [5], as shown in Fig. 1(g) and (h); these lead to new considerations.

Providing the maximum lever arm results in exposure of the steel element to compressive forces which may induce local buckling of the steel (although the possibility is always greater when the steel is acting alone), something that is avoided when using the encased steel beam. To provide both a large

* Corresponding address: Imperial College of Science, Technology and Medicine, Department of Civil and Environmental Engineering, London SW7 2BU, United Kingdom. Tel.: +44 20 7594 6097; fax: +44 20 7594 6049.
E-mail address: d.nethercot@ic.ac.uk (D.A. Nethercot).

0141-0296/$ - see front matter © 2006 Elsevier Ltd. All rights reserved.
doi:10.1016/j.engstruct.2006.04.010

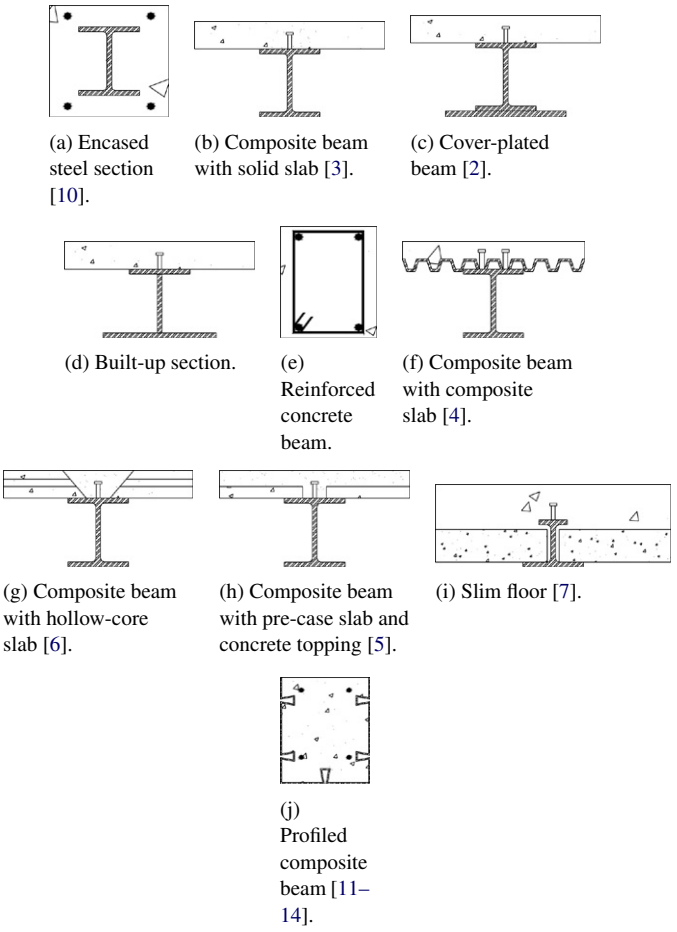

(a) Encased steel section [10].
(b) Composite beam with solid slab [3].
(c) Cover-plated beam [2].
(d) Built-up section.
(e) Reinforced concrete beam.
(f) Composite beam with composite slab [4].
(g) Composite beam with hollow-core slab [6].
(h) Composite beam with pre-case slab and concrete topping [5].
(i) Slim floor [7].
(j) Profiled composite beam [11–14].

Fig. 1. Steel–concrete composite cross-sections.

eccentricity and protection against local buckling, a slim-floor system was introduced, comprising a steel beam encased either fully or partly within the slab. Such a configuration, which is shown in Fig. 1(i), allows greater concrete width and the provision of an asymmetric beam compared to the conventional encased beam of Fig. 1(a) [7].

The use of cold-formed steel is attractive, as it can provide permanent form-work and integral shuttering to the concrete section. In addition to the profiled composite slab, cold-formed sheeting has been used to form the profiled composite beam, as shown in Fig. 1(j), which can be considered as one of the most recent developments in steel–concrete composite beam construction [11–14].

1.1. Design consideration of a steel–concrete composite beam

In common with the design of any structural member, a steel–concrete composite beam must be designed to satisfy both serviceability and ultimate requirements. For the former, design checks are made against deflection and vibration etc. The most important elastic property of the composite cross-section is its second moment of area, which requires transformation of the cross-section into a single unit so as to allow both elements, concrete and steel, to have a similar elastic response. Based on the full interaction assumption, this is done by multiplying or dividing the area of one of the elements by the modular ratio,

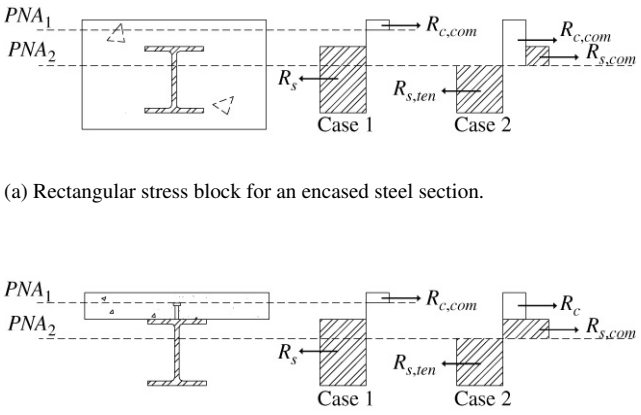

(a) Rectangular stress block for an encased steel section.

(b) Rectangular stress block for a conventional composite beam.

Fig. 2. Rectangular stress block distribution for composite beams.

α_e, which is the ratio between the base element's modulus of elasticity, E_b, and the modulus of elasticity of the other element, E_e. The calculation must also consider whether the concrete is cracked or uncracked.

When satisfying the ultimate strength requirements, several aspects of behaviour require checking. Herein, only the ultimate moment capacity is considered. When determining this, the rectangular stress block method is usually adopted. In this approach, an element is assumed to be either fully stressed or unstressed. Cross-sectional equilibrium is established between the steel, concrete, reinforcement and shear connection resultants (if appropriate), and consideration is given to the location of the plastic neutral axis, location of the points of action of the resultant forces, and the magnitude of the lever arms. The resultant force in each element is taken as the product of the material strength and the relevant area; it is assumed to act at the centroid of the stress block. The ultimate moment capacity is then obtained as the summation of the first moment of these resultants about any reference point or level. Fig. 2 shows the ultimate condition and the stress blocks for an encased steel section and a composite beam with a solid slab for the full shear connection condition. R_c and R_s denote the concrete and steel resultant forces, and subscripts ten and com refer to tension and compression, respectively. *PNA* means plastic neutral axis. There are several possible locations for the PNA: either above the steel section or in the steel upper flange or in the steel web. If the PNA lies above the steel section, both cross-sections will have similar stress profiles but, of course, with different magnitudes. However, if the PNA falls within the steel section then, for the encased steel section, overlapping of the stress profiles occurs. Such an overlap indicates that the PNA crosses both the steel and the concrete element, and complicates the determination of the location of the PNA.

1.2. PCFC beam

Currently, the authors are developing a new type of composite beam known as a Pre-cast Cold-formed Composite

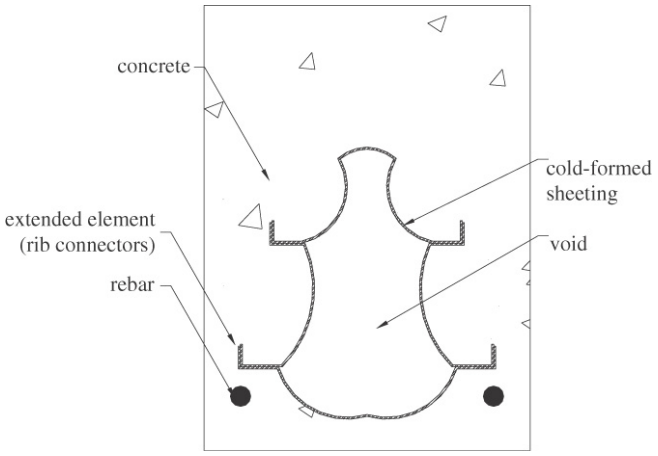

Fig. 3. Cross-section of PCFC beam.

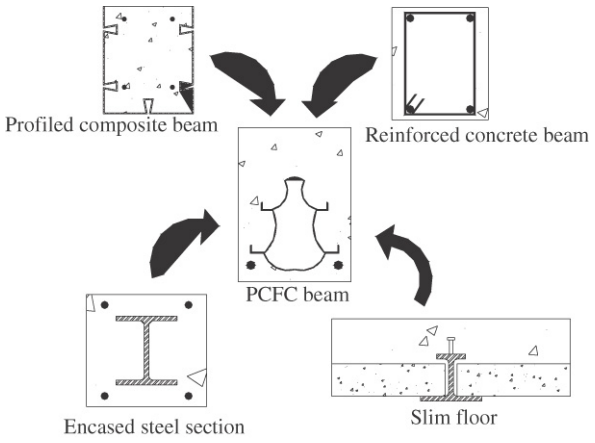

Fig. 4. Sources of evolution of the PCFC beam.

Beam, or PCFC beam. The beam consists of a closed cold-formed steel section encased in reinforced concrete. A possible cross-section is illustrated in Fig. 3. Such a configuration can be considered as a further evolution of the profiled composite beam shown in Fig. 1(j) for which the additional benefits are:

(i) The cold-formed sheeting provides a hollow core for the beam and is no longer located at the perimeter of the concrete section; therefore, the eccentricity between resultants can be adjusted without affecting the beam's outer section.
(ii) Since the cold-formed steel contains no concrete, it does not have to be present throughout the depth of the beam, thus reducing the exposure of the steel to compressive stresses. Also, the rigid medium provided by the concrete allows only one-way buckling, a benefit also shared by the profiled composite beam.
(iii) The encasement eliminates any bearing problem of the cold-formed steel due to the introduction of the load.
(iv) The hollow core can act as a service duct.

The arbitrary shape of the steel section is chosen deliberately to emphasize the freedom in geometry that is available when using cold-formed steel sections. From the composite beam point of view, this freedom allows for optimization by matching the supply and demand based on the composite beam concept. The extended steel elements are not only part of the steel element but also act as 'L-rib' connectors, making external shear connectors unnecessary. Although PCFC beams may not exhibit the advantage of providing the permanent formwork of a profiled composite beam, the prefabricated nature of the beam may be retained by using pre-cast concrete.

Obviously, the PCFC beam also resembles the encased steel beam and the slim floor type of composite beam. Besides the void, the PCFC beam differs from the other two by the use of a cold-formed section instead of a hot-rolled or built-up section. Cold-formed sections provide more options in terms of shape. Also, since the cold-formed section is relatively thin, then the 'over-reinforced' condition, if not desired, can be more easily avoided.

At the other extreme, the PCFC beam can be considered as evolving from a conventional reinforced concrete beam. In this, the role of the concrete in tension is essentially to hold the reinforcement in place. The cold-formed steel section in a PCFC beam replaces the reinforcement bars of the conventional reinforced concrete beam, but the void that is created reduces the amount of concrete in tension.

The evolution of the PCFC beam from its four sources is shown in Fig. 4. However, based on Fig. 3, it is to be expected that the design of a PCFC beam will be more complex than is the case for most of the beams shown in Fig. 1.

The first complication arises from the absence of rectangularity for the cross-section. The void, the corners and the irregular steel shape are the cause of this irregularity. Also, the stretching of the sheeting during the forming process creates nonuniform thicknesses between corners and flat regions. The immediate effects of these are difficulties in determining the action point of the force resultants for the various components and in transforming the components into a single unit (required to evaluate the cross-sectional properties used for the serviceability checks).

The hybrid properties of cold-formed steel are the next complication. To incorporate the higher strength at the corners in design, these elements need to be treated individually, increasing the scope of the problem. The simple assumption of average values, on the other hand, reduces the effectiveness of the cold-formed steel.

The third complication is due to overlapping between the steel and concrete elements except in the upper part of the beam. If the plastic neutral axis locations intersect both the steel and concrete elements, the determination of the location of the plastic neutral axis requires an iteration process. Partial shear connection introduces a further complication.

1.3. Objectives of the paper

Based on the foregoing discussion, the objectives of this paper are:

(i) to develop a general procedure for the determination of the cross-sectional properties of complex beam cross-sections, such as the PCFC beam, that is systematic and suitable for computer-aided calculation;

(ii) to use this procedure to compare the flexural performance of the proposed PCFC beam with that of a similar profiled composite beam.

2. Design basis of PCFC beam

The key feature of the procedure is the use of functions to describe the shape of the elements in a cross-section (definitions of elements and function are given in Sections 3.3 and 3.4), leading to the determination of the cross-sectional properties through appropriate integrations. This is presented symbolically, since it is intended for computer-aided calculation. Such a procedure has the following advantages:

(i) A systematic procedure reduces calculation and thus reduces the possibility of clumsy errors.
(ii) A computerized procedure provides the basis for a rapid design when passing through the various design checks.
(iii) A procedure that is both systematic and computerized encourages a comprehensive analysis without the need to simplify the problem (as was inevitably the case for the design of profiled composite slabs and profiled composite beams when using existing approaches).
(iv) The proposed procedure is suitable for mass-production manufacturers where products are materially similar but different in scale and shape.

The design basis for the PCFC beam described herein (but which is also sufficiently general for use on other complex beam cross-sections) is developed for a beam in positive bending. It covers the determination of the second moment of area of the cross-section, assuming full interaction and the ultimate moment capacity of the beam for both full and partial shear connection conditions.

2.1. Physical and application stages

The procedure is presented in two stages: the *physical stage* and the *application stage*. The *physical stage* deals with the identification of the physical components of the cross-section, their definitions, and their subsequent representation by symbolic expressions. The *physical stage* provides the understanding, including identifying the required data and how to input them. It provides guidance on exactly how to break down the complex cross-section into discrete entities which later can be prescribed in matrix form. The *application stage* represents these with standard mathematical formulations, arranged to suit computer programming; this stage is intended for the implementation. Thus the concepts developed in the *physical stage* underpin the mathematical formulations of the *application stage*. A detailed discussion of both stages is given in Sections 3 and 4 of this paper.

2.2. Design assumptions

The procedure is based on the assumption that beam design is governed by flexure, thus shear-related failures are not considered. Also, it is assumed that local buckling does not occur in the steel elements. The latter assumption holds true in most cases because of the enhancements provided by the configuration of the cross-section, i.e. only one-way local buckling is possible, and the location of the neutral axis is most likely to be relatively high, leaving only a small amount of steel in compression. Should the neutral axis lie above the steel section, then there will be no possibility for local buckling.

The procedure is also based on the assumptions inherent in standard composite beam design, listed as follows:

(i) Steel elements are assumed to be fully stressed to their design strength, p_y, in both tension and compression, and concrete elements are assumed to be stressed to a uniform compressive stress of $0.85 f_c$ throughout the compression depth.
(ii) Concrete in tension has negligible strength and is thus neglected.
(iii) Slip is insignificant (full interaction assumption).
(iv) Plane sections remain plane.

2.3. Approximation error

Approximation errors will occur if the chosen function does not describe the shape of an element exactly. Suitable functions are proposed in Section 3.4.

3. Physical stage

This stage is concerned with the identification of the physical components of the cross-section, their definition and symbolic expression; it has the following components:

(i) symmetricality;
(ii) strips;
(iii) elements;
(iv) functions;
(v) geometrical points.

3.1. Symmetricality

Since the great majority of composite beam cross-sections, especially the forms for which this process has been devised, are symmetrical about their minor axis, the following development is based on this assumption. It permits significant simplifications to be made.

3.2. Strips

The cross-section is first discretized into a total of S rectangular strips, as shown in Fig. 5. Individual strips are numbered from 1–S, with a typical strip being referred to as strip s. Each strip may contain a mix of:

(i) *line elements*;
(ii) *bar elements*;
(iii) *area elements*.

Each of these is then represented by a 1-rule continuous function, as explained in Section 3.4. The different types of elements are described below.

3.3. Elements

An *area element*, a typical example of which is identified in Fig. 5, is defined as having significant dimensions in both

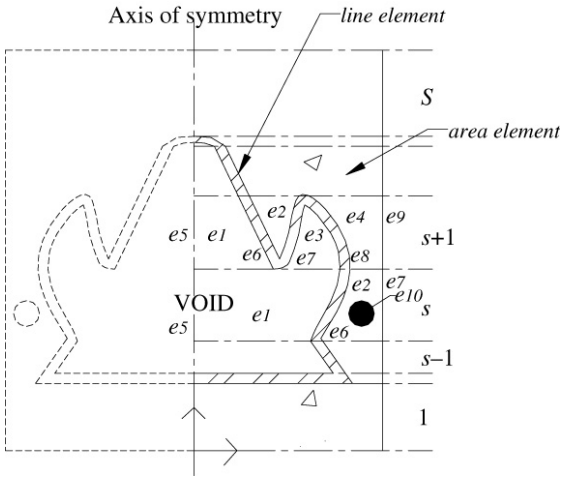

Fig. 5. Discretization of a cross-section into S strips.

directions. In comparison, a *line element*, an example of which is shown in Fig. 5, is defined as having insignificant dimensions in one direction compared to the other. *Bar elements* have negligible size, are assigned only axial properties, and are used to represent reinforcement. Thus, in general, *area elements* are used to represent thick materials such as concrete, while *line elements* are employed to represent thin materials such as thin plate, steel sheeting or composite fibres.

Elements are also regarded as either *active* or *passive*. *Active* elements contribute to the stiffness and strength of the cross-section, while *passive* elements do not. Thus a void, which is considered as an *area element*, is prescribed as *passive*. A *line element* representing a boundary is also described as *passive*, since it does not contribute to either the stiffness or the strength of the cross-section.

The process of defining and numbering elements within a strip may best be appreciated by referring to a specific example. Consider strip $s+1$ of Fig. 5. This contains *area elements* e_1 and e_3 prescribed as *passive* since they are voids, *area elements* e_2 and e_4 prescribed as *active* since they consist of concrete, *line elements* e_5 and e_9 prescribed as *passive* since they form internal and external boundaries of the strip, and *line elements* e_6, e_7 and e_8 prescribed as *active* since they represent steel sheeting. Strip s contains a mix of *active* and *passive area elements*, *active* and *passive line elements* and the *bar element* e_{10}, representing a reinforcing bar.

It is also important to observe certain rules when deciding on the numbering system for elements. This should follow the sequence *area elements*, followed by *line elements*, followed by *bar elements*. It also necessary to preserve the same group of numbers for the same class of element, i.e. to identify the maximum number of area elements within any one strip, to ensure that all *area elements* in other strips are numbered from this group and *that line elements* and *bar elements* are numbered from other groups. Referring again to Fig. 5, it is clear that strip $s+1$ contains the largest number of *area elements* and *line elements*. Since any *area element* must be contained within two *line elements*, if there are f *area elements* within a strip, then it follows that there must also be $f+1$ *line elements* within that same strip. Thus the value of f obtained from the strip with the largest number of elements becomes the governing factor for subscript numbering for the whole cross-section. *Area elements* are then referred to as $e_{e\leq f}$ and *line elements* are referred to as $e_{e>f}$, where $e = 1, 2, 3, \ldots$ and, for any *line element*, it is understood that the subscript e cannot be greater than $2f+1$. Since *bar elements* are numbered last, and adopting the subscript g for this class, their range can be stated as $2f+1 < g \leq G$, in which G is the total number of elements existing in that particular strip.

Referring once again to strip $s+1$ in Fig. 5, which is already identified as the strip having the largest number of *area* and *line elements*, the value of f (and thus f for the whole cross-section) is 4. Thus *area elements* are denoted as e_1–e_4 and *line elements* as e_5–e_9, with elements closest to the axis of symmetry being numbered first. Once this has been recognized, an arbitrary value may be decided for G, providing that it is sufficiently large to accommodate all the previously identified *area elements* and *line elements* within the most populated strip and then leaves some space for a reasonable presence of *bar elements* within other strips. Referring to strip s of Fig. 5, it has only two *area elements* and three *line elements*. Thus the former are designated e_1 and e_2 (with e_3 and e_4 unused), the *line elements* are designated as e_5–e_7 (with e_8 and e_9 unused), and the single *bar element* is set as e_{10} (with e_{11} set to 0). Continuation of this process for the whole cross-section allows it to be represented by a matrix of S by G components. For the example of Fig. 5, $S = 8$ and G has been chosen as 11, leading to the matrix representation of Fig. 6. Any element within this matrix is designated as $e_{s,e}$, where subscripts s and e, which represent the row and column number of the matrix, refer to the numbering of the strips and elements, respectively.

strips\elements	1	2	3	4	5	6	7	8	9	10	11
1	$e_{1,1}$	0	0	0	$e_{1,5}$	$e_{1,6}$	0	0	0	0	0
2	0	0	0	0	$e_{2,5}$	0	0	0	0	0	0
3	$e_{3,1}$	$e_{3,2}$	0	0	$e_{3,5}$	$e_{3,6}$	$e_{3,7}$	0	0	0	0
4	$e_{4,1}$	$e_{4,2}$	0	0	$e_{4,5}$	$e_{4,6}$	$e_{4,7}$	0	0	$e_{4,10}$	0
5	$e_{5,1}$	$e_{5,2}$	$e_{5,3}$	$e_{5,4}$	$e_{5,5}$	$e_{5,6}$	$e_{5,7}$	$e_{5,8}$	$e_{5,9}$	0	0
6	$e_{6,1}$	$e_{6,2}$	0	0	$e_{6,5}$	$e_{6,6}$	$e_{6,7}$	0	0	0	0
7	$e_{7,1}$	0	0	0	$e_{7,5}$	$e_{7,6}$	0	0	0	0	0
8	$e_{8,1}$	0	0	0	$e_{8,5}$	$e_{8,6}$	0	0	0	0	0

Fig. 6. The matrix representation of element notation in a cross-section (given in Fig. 5).

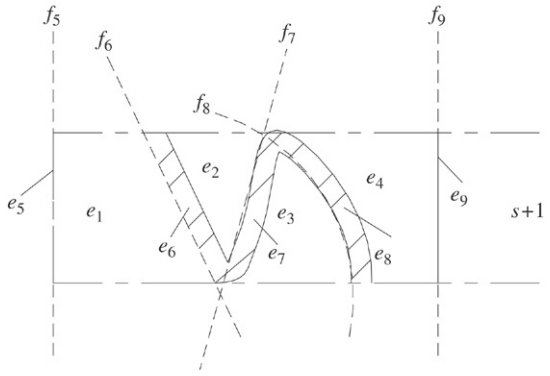

Fig. 7. Strip $s + 1$ of Fig. 5.

3.4. Functions

The function used to represent a *line element* must be a 1-rule continuous function and must span the height of the strip throughout. Using a Cartesian coordinate system, the bottom-left corner of the strip is taken as the origin. The independent variable of the function is the symmetrical axis direction, y. Observing the rules of Section 3.3, the function is abbreviated as $f_{e>f}(y)$. A function may be exact or an approximation, depending on the complexity of the actual shape of the *line elements*. For example, as shown in Fig. 7, which refers to strip $s + 1$ of Fig. 5, f_5 and f_9 are constants and f_6 is a linear function, while f_7 and f_8 can be approximated (say) by a linear expression and a polynomial expression, respectively. However, for one particular condition, the function cannot be expressed in terms of the symmetrical axis direction. This occurs when a straight *line element* or a series of *line elements* is positioned perpendicularly to the y-axis, for example element $e_{2,5}$ in Figs. 5 and 6. As an approximation, however, such *line elements* may still be represented by treating the *line element* as being very slightly inclined with respect to the x-axis, as shown in Fig. 8. The element is then expressed as having a gradient of l_e/t_e, where l_e is the element's length and t_e is the element's thickness. Using the approach outlined in Section 3.3, the complete set of functions can be arranged into a matrix, termed the FE matrix. Since functions relate directly to *line elements*, the first f columns and the last g columns of the matrix will be filled with null elements.

3.5. Geometrical heights

Geometrical heights define element size and location. The two types are illustrated in Fig. 9 as:

(i) *local height*;
(ii) *global height*.

Abbreviated as y_n, *local height* is the depth of the strip. For a *bar element*, the *local height*, y_b, is taken as the depth of the bar from the bottom of the strip. The *global height*, z_n, is required for calculations at cross-sectional level and is the vertical distance of the bottom of the strip from the x-axis. Since geometrical heights y_n and z_n belong to a strip, they can be represented as a vector of S components.

4. Application stage

The *application stage* develops the mathematical formulations to suit computer programming. The formulations are set-up in a discrete manner in line with the matrix nature of the *physical stage*. The *application stage* has the components:

Elemental

(i) area of element;
(ii) centroid of element;
(iii) transformed area of element;
(iv) element second moment of area;
(v) element resistances.

Cross-sectional

(vi) centroid of beam (location of elastic neutral axis (ENA));
(vii) second moment of area of uncracked section;
(viii) second moment of area of cracked section;
(ix) plastic moment capacities.

4.1. Area of element

The area of an *area element* is obtained as:

$$A_{e\leq f} = \int_0^{y_n} \int_{f_{e+f}+t_{e+f}}^{f_{e+f+1}} \mathrm{d}x\,\mathrm{d}y \tag{4.1}$$

while the area of a *line element* is obtained as:

$$A_{e>f} = \left(\int_0^{y_n} \sqrt{1 + \left(\frac{\mathrm{d}f_e}{\mathrm{d}y}\right)^2}\,\mathrm{d}y \right) t_e \tag{4.2}$$

where t is the thickness of the *line element* and f_{e+f} and f_{e+f+1} are the functions of two successive *line elements* bordering *area element* e_e.

The area of a *bar element* is defined as:

$$A_g = \pi r_g^2 \tag{4.3}$$

where r_g is the radius of the *bar element*.

4.2. Centroid of element

The height of the centroid of an element in a strip, y_e, is measured from the bottom of the strip. The height of the centroid of an *area element* is defined as:

$$y_{e\leq f} = \frac{\int_0^{y_n} \int_{f_{e+f}+t_{e+f}}^{f_{e+f+1}} y\,\mathrm{d}x\,\mathrm{d}y}{A_{e\leq f}} \tag{4.4}$$

while the height of the centroid of a *line element* is approximated as:

$$y_{e>f} = \frac{y_n}{2}. \tag{4.5}$$

The height of the centroid of a *bar element* y_g is also its *local height*, y_b.

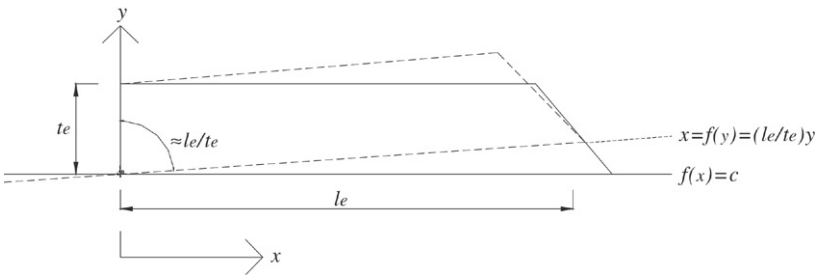

Fig. 8. Approximation for $f(x) = c$.

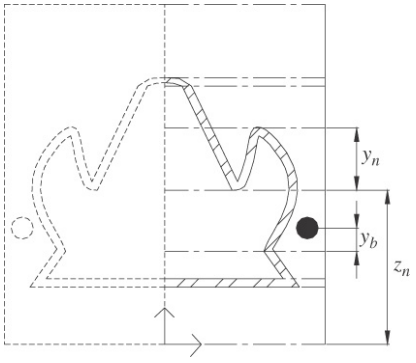

Fig. 9. Geometrical heights.

4.3. Transformed area of element

The determination of the second moment of area of a composite beam requires the transformation of the cross-section into a single unit. This ensures that each element has similar elastic properties. Based on the full interaction assumption, this is done by multiplying or dividing the element's area by a modular ratio, α_e, which is the ratio between a base element's modulus of elasticity, E_b, and the modulus of elasticity of the element, E_e. The modular ratio, α_e, is given as:

$$\alpha_e = E_b/E_e \tag{4.6a}$$

$$\alpha_e = E_b k/E_e \tag{4.6b}$$

where k is a factor that takes into account long-term effects, e.g. shrinkage, creep.

It is efficient to apply α_e to the x-parallel dimension of an element, as this will not affect the height of the element's centroid, y_e, derived previously. The highest value of E_e among the materials in a strip is chosen as the base element's modulus of elasticity, E_b, because this will ensure that the effective area of all material will be reduced, except, of course, for the base material itself, where the area will be unchanged.

The determination of the effective area of an *area element* in a strip requires the shifting of the relevant function by x_α. The shifted function is now the combination of

$$f_{e>f} + x_\alpha \tag{4.7}$$

where x_α is given as:

$$x_\alpha = f_{e+f+1} - \left(f_{e+f} + t_{e+f}\right) - \left(\frac{f_{e+f+1} - \left(f_{e+f} + t_{e+f}\right)}{\alpha_{e\leq f}}\right). \tag{4.8}$$

4.4. Second moment of area of element

The second moment of area of an *area element* taken about the bottom of the strip is defined as:

$$I_{e\leq f,\text{bot}} = \int_0^{y_n} \int_{f_{e+f}+t_{e+f}+x_\alpha}^{f_{e+f+1}} y^2 \,\mathrm{d}x\,\mathrm{d}y \tag{4.9}$$

while the second moment of area of a *line element* taken about the bottom of the strip is defined as:

$$I_{e>f,\text{bot}} = \left(\int_0^{y_n} \sqrt{1 + \left(\frac{\mathrm{d}f_e}{\mathrm{d}y}\right)^2}\, y^2 \,\mathrm{d}y\right) \frac{t_e}{\alpha_e}. \tag{4.10}$$

As an axial element, a *bar element* does not have a second moment of area of its own.

The second moment of area of an element taken about the element's centroid is defined as:

$$I_{e,\text{cen}} = I_{e,\text{bot}} - \frac{A_e}{\alpha_e} y_e^2 \tag{4.11}$$

where the subscripts bot and cen refer to bottom and centroid, respectively.

4.5. Element resistances and strip resistance

Based on the rectangular stress block method, an element's resistance is taken as the product of the element's area and the material design strength, and is given as:

$$P_e = 2A_e f_{e,y} \tag{4.12}$$

where $f_{e,y}$ is the design strength of element e. Safety factors may be imposed on the material strength. The element resistance is assumed to act at the centroid of the corresponding element.

However, in taking into account the sensitivity of some types of element to stress direction, a factor $\phi_{e,c/t}$ is imposed on Eq. (4.12), resulting in the following:

$$P_{e,c/t} = 2A_e \phi_{e,c/t} f_{e,y}. \tag{4.13}$$

The subscripts c and t refer to compression and tension, respectively, while subscripts ',' and '/' refer to 'and' and 'or',

respectively. Such a formulation is intended for materials such as concrete, for which the strength in tension is neglected. Therefore, for most cases, $\phi_{e,c}$ can be taken as unity.

Strip resistance is the total of the element resistances within the strip. To take into account the sensitivity to stress direction, the strip resistance is again categorized into:

(i) compressive strip resistance, $R_c = \sum P_{e,c}$ (4.14a)

(ii) tensile strip resistance, $R_t = \sum P_{e,t}$. (4.14b)

4.6. Centroid of beam

The determination of the centroid of a cross-section also locates the position of the elastic neutral axis since, under the elastic and full interaction assumption, both points are coincident.

The centroid of the cross section, Y, measured from the x-axis is defined as:

$$Y = \frac{\sum_{s=1}^{S} A_e\,(y_e + z_n)}{\sum_{s=1}^{S} A_e}. \tag{4.15}$$

4.7. Second moment of area of beam (uncracked section)

The second moment of area of an uncracked section, $I_{x,\mathrm{un}}$, about the centroid of the beam parallel to the x-axis is determined using the Parallel Axes Theorem. This is defined as:

$$I_{x,\mathrm{un}} = 2\sum I_{e,\mathrm{cen}} + \frac{A_e}{\alpha_e} d_e^2 \tag{4.16}$$

where the subscript 'un' refers to uncracked. For an element having its centroid higher than or coincident with the centroid of the cross-section (i.e. $y_e + z_n > Y$),

$$d_e = z_n - Y + y_e. \tag{4.17a}$$

For an element having its centroid lower than the centroid of the cross-section, (i.e. $y_e + z_n < Y$)

$$d_e = Y - y_e - z_n. \tag{4.17b}$$

4.8. Second moment of area of beam (cracked section)

For a cracked concrete section, the elastic neutral axis (ENA) no longer coincides with the centroid of Eq. (4.15). The determination of the location of the ENA can be carried out by equating the first moment of area between the 'upper' region and the 'lower' region of the cross-section. This requires an iteration process to locate the strip within which the ENA falls. However, this is thought to be unnecessary, as the exact location of the ENA will most likely remain close to the centroid and a simplified approach is adopted here. (A full procedure involving iteration is devised for the plastic neutral axis (PNA) later.)

Therefore, for the determination of the second moment of area of the cracked concrete section, $I_{x,\mathrm{cr}}$, it is assumed that the ENA and the centroid of Eq. (4.15) remain coincident. $I_{x,\mathrm{cr}}$ is thus taken as $I_{x,\mathrm{un}}$, with the second moment of area of the concrete in tension subtracted from it. By assuming that the centroid of the beam lies in strip q, and if all active *area elements* are concrete elements, the second moment of area of a cracked section, $I_{x,\mathrm{cr}}$, about the centroid of the beam parallel to the x-axis is obtained as:

$$I_{x,\mathrm{cr}} = I_{x,\mathrm{un}} - 2\left(\sum_{s=1}^{s=q-1} I_{e\le f,\mathrm{cen}} + \frac{A_{e\le f}}{\alpha_{e\le f}}(Y - y_e - z_n)^2\right) - 2\left(I_{e\le f,\mathrm{cen}} + \frac{A_{e\le f}}{\alpha_{e\le f}}(Y - y_e - z_n)^2\right)_{q,t} \tag{4.18}$$

where the subscript 'cr' refers to cracked. The first bracket contains concrete terms extracted from strips lower than strip q and the second bracket contains concrete terms in tension for strip q. All the terms in the first bracket have been calculated previously as Eqs. (4.1) and (4.4). These equations are also reused to determine the terms in the second bracket by replacing the upper integration limit in the y-direction, y_n with $Y - z_n$.

4.9. Plastic moment capacities

The plastic moment capacity of a composite beam is calculated using the rectangular stress block approach. The ultimate condition of the beam is governed by the degree of shear connection, defined as the ratio of the longitudinal shear strength provided compared to that required for full shear connection. Herein, the determination of the plastic moment capacity of the composite beam is explained first for the general case of partial shear connection and is then specialized for the two extreme cases, i.e. full and zero shear connection.

In a conventional steel–concrete composite beam, partial shear connection occurs when the resultant force from the shear connectors, termed F_b, is smaller than the weaker of the axial resistance of the concrete section or the steel section, respectively termed F_c and F_s. F_c and F_s are obtained as the product of the material strength and the whole cross-sectional area of the concrete or the steel. Such easy checking of the partial shear connection condition is possible because the concrete and the steel elements are placed at different levels, as shown in Fig. 10(a) for a beam in positive bending. The condition requires that, to obtain the full shear connection condition, at least one material must have fully yielded in one direction. Although there can be two full shear connection conditions, i.e. PNA in the concrete or in the steel, because both elements must yield in both directions there is a unique partial shear connection condition for the beam, as shown in the figure, and since neither of the elements yields completely in one direction, there exists two locations for the plastic neutral axis (PNA).

In a profiled composite beam, on the other hand, the elements are placed largely at the same level, thus making such a check impossible because, even for the full shear connection condition, each element is subjected to both compression and

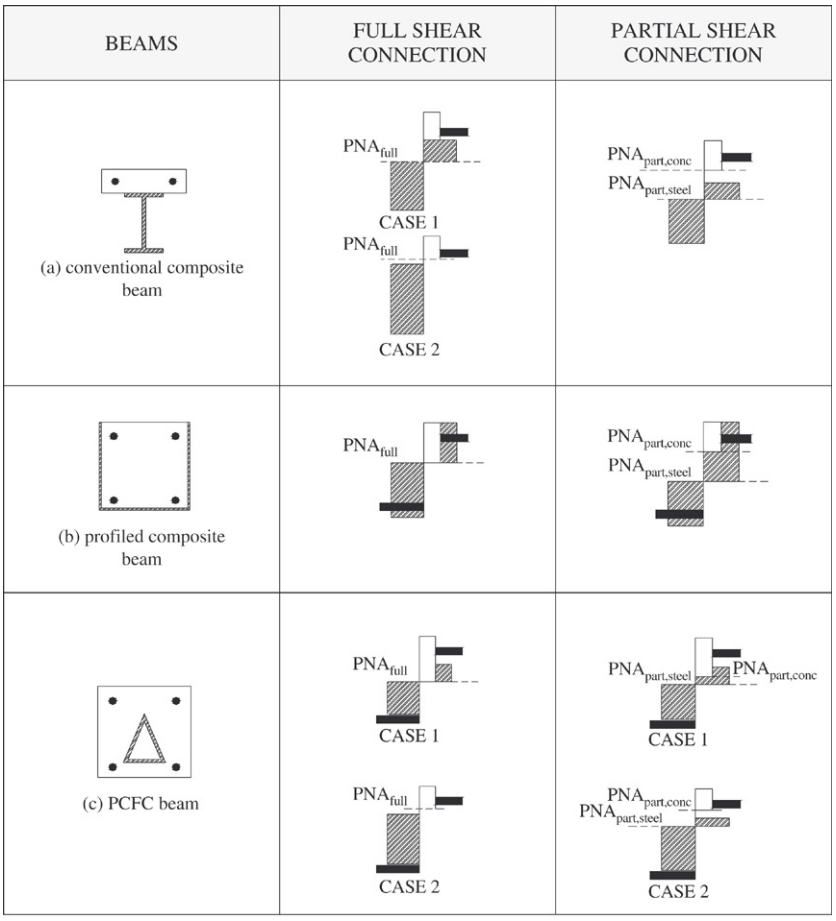

Fig. 10. Possible equilibrium conditions of composite beams.

tension. The systematic approach for determining the level of partial shear connection is to first calculate the minimum longitudinal shear resultant required to achieve full shear connection, $F_{b,\min}$, and to compare it with the value of F_b provided; this step will be illustrated later. But a condition that always prevails for the partial condition is that the concrete resultant force, $F_{c,\mathrm{com}}$, will always be smaller than the value required for full shear connection. In Fig. 10(b), $F_{c,\mathrm{com}}$ is the resultant force for the smaller white rectangular stress block. This is an important observation which will be used in determining the minimum longitudinal shear resultant, $F_{b,\min}$.

In a PCFC beam, there are two possible locations for the PNA for the full shear connection condition, since the PNA can be in either the upper part of the concrete section or the steel section, and there are also two possible partial shear connection conditions, as shown in Fig. 10(c). Despite the various possible shapes for the stress block, the force distributions are similar for all beams, as given in Fig. 11.

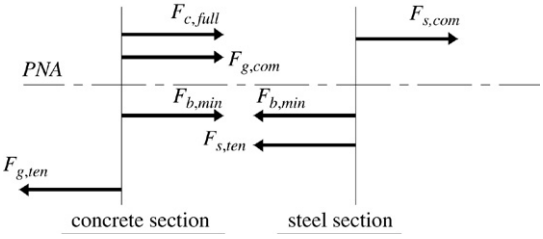

(a) Distribution of forces for full shear connection.

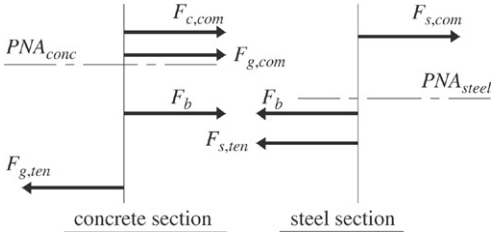

(b) Distribution of forces for partial shear connection.

Fig. 11. Distribution of forces in a composite beam.

4.9.1. Minimum longitudinal shear force for full shear connection — $F_{b,\min}$

To determine whether a beam exhibits the partial shear connection condition, a check can be made against the minimum resultant longitudinal shear force, termed $F_{b,\min}$ and defined as the minimum value necessary for full shear connection. If F_b provided is less than the calculated $F_{b,\min}$, then partial shear connection exists. This single check is sufficient for a profiled composite beam, since there is a unique

full shear connection condition for the beam. For a PCFC beam, however, since Case 2 for full shear connection resembles the condition of the conventional composite beam, F_b must in addition be less than the steel axial resistance F_s.

An established approach to determining $F_{b,\min}$ is to equate the location of the PNA in the concrete section to the location of the PNA in the steel section. This approach has been outlined by Oehlers et al. [12]. Their argument is that, since, in this type of beam, the full shear condition and full interaction are not distinguishable, at these conditions slip strain must be zero and hence the PNA in both elements must be coincident. This approach is suitable for their simplified arrangement, since there is only one possible location for the PNA, i.e. within the depth of the steel web. In the present procedure, since there are more possibilities for the location of the PNA due to the discretization of the cross-section into strips, a different approach for the determination of $F_{b,\min}$ is adopted.

Since the plastic moment capacity of a composite beam with partial shear connection cannot exceed the capacity obtained for full shear connection, the latter condition requires that all elements must have yielded, since the presence of any unyielded portion of material would imply a possibility for the capacity to increase. Examining this by referring to Fig. 12, which shows the force distributions in both the concrete section and steel section for full and partial shear connection, identifies eight force components as follows:

- $F_{c,\text{full}}$ is the concrete section compressive resistance for the full shear condition;
- $F_{c,\text{com}}$ is the concrete section compressive resistance for the partial shear condition;
- $F_{g,\text{com}}$ is the compression resistance of the rebar for both full and partial shear conditions;
- $F_{g,\text{ten}}$ is the tension resistance of the rebar for both full and partial shear conditions;
- $F_{b,\min}$ is the minimum longitudinal shear resultant force required to achieve the full shear connection condition;
- F_b is the longitudinal shear connection resultant actually provided $= \tau_b S_r n_r L$
  where τ_b is the rib shear strength, S_r is the interface perimeter (as shown in Fig. 12), n_r is the number of ribs in the cross-section, and L is the distance of the critical cross-section from the support or the point of contraflexure.
- $F_{s,\text{com}}$ is the steel section compressive resistance for full or partial shear conditions;
- $F_{s,\text{ten}}$ is the steel section tension resistance for full or partial shear conditions.

For both connection conditions, it can seen that $F_{g,\text{com}}$ and $F_{g,\text{ten}}$ have fixed magnitudes, based on the assumption that rebar is always fully yielded. Thus, this leaves only two components in the concrete section, $F_{c,\text{full}}$ and $F_{b,\min}$ for the full shear connection condition and $F_{c,\text{com}}$ and F_b for the partial shear connection condition; any change in the magnitude of one will affect the other. Since any reduction in F_b from its limit $F_{b,\min}$ will reduce $F_{c,\text{com}}$ from its limit $F_{c,\text{full}}$, $F_{b,\min}$ is thus the

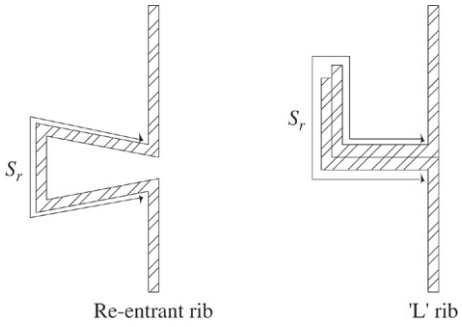

Fig. 12. Shape/perimeter of ribs.

force required for the concrete section to obtain its maximum resultant $F_{c,\text{full}}$, which in turn depends on the unique concrete crushing depth, i.e. the location of the PNA at the full shear connection condition. Based on this, $F_{b,\min}$ can be calculated by determining first the location of the PNA for this full condition.

The determination of the location of the PNA for the full shear connection condition requires an iteration process. As mentioned in Section 1.1, for a conventional composite beam, there are three possible locations for the PNA: in the concrete section, in the upper steel flange or in the steel web. For a PCFC beam, there are more options, so it is necessary to derive an algorithm to drive the iteration process for locating the strip within which the PNA lies. PNA falls in strip p when:

$$\sum_{s=S-k+1}^{S} (R_c)_s > \sum_{s=1}^{S-k} (R_t)_s \tag{4.19}$$

where $p = S - k_h + 1$ and k_h is the kth attempt in which Eq. (4.19) is satisfied.

Based on Eq. (4.19), it can be seen that the determination for strip p depends on k_h, which is the cycle number of the iteration needed in satisfying Eq. (4.19). The application of Eq. (4.19) is illustrated in Example 2. Once the strip in which the PNA falls has been identified, the exact location of the PNA can be determined. The height of the PNA measured from the bottom of strip p, h_f can be obtained by solving the following equality:

$$\sum_{i=0} (R_c)_{p+i+1\le S} + \left(\sum P_{e,c}\right)_{p,c} = \sum_{i=0} (R_t)_{p-i-1\ge 1} + \left(\sum P_{e,t}\right)_{p,t} + \left(\sum P_g\right)_p \tag{4.20}$$

in which $\left(P_{e,c}\right)_{s,c}$ and $\left(P_{e,t}\right)_{s,t}$ are the partial element resistances in strip p, being separated by the PNA. These partial values can be determined by the reuse of Eqs. (4.1) and (4.2), substituting the integration limit in the y-direction, y_n, by $y_n - h_f$ and h_f for the compressive part and the tensile part, respectively.

Once h_f is determined, $F_{b,\min}$ can be determined as follows. Eq. (4.20) actually expresses the internal equilibrium of the whole cross-section, not distinguishing elements or materials. An individual equilibrium of, say, the concrete section can be obtained by extracting the terms containing *area elements* and *bar elements* from Eq. (4.20). The residual resultant of

the extracted terms is then balanced by an equal resultant force in the opposite direction, contributed by the composite action. Since this resultant is the force required for the concrete section to maintain its full shear connection equilibrium, this countering resultant is therefore the desired $F_{b,\min}$, which can now be given as:

$$F_{b,\min} = \sum_{i=0} \left(P_{g,t}\right)_{p-i-1\geq 1} + \left(\sum P_g\right)_p - \sum_{i=0} \left(P_{g,c}\right)_{p+i+1\leq S} - \sum_{i=0} \left(P_{e\leq f,c}\right)_{p+i+1\leq S} - \left(\sum P_{e\leq f,c}\right)_{p,y_p-h_f}. \quad (4.21)$$

Eq. (4.21) states that $F_{b,\min}$ is equal to the residual between the compressive forces and the tensile forces in the concrete section. The fourth term on the right-hand side of the equation, $\left(\sum P_{e\leq f,c}\right)_{p,y_p-h_f}$, represents the partial compressive resistance of strip p. The height of the compressive region of strip p is given by the subscripts $y_p - h_f$, where y_p is the local height of strip p and h_f is the height of the PNA measured from the bottom of strip p, a known value. If the first two terms on the right-hand side of the equation are represented as $F_{g,\text{ten}}$, the third term as $F_{g,\text{com}}$ and the last two terms as $F_{c,\text{full}}$, then Eq. (4.21) actually expresses the equilibrium condition of the concrete section of Fig. 11(a). Based on Eq. (4.21), $F_{b,\min}$, and thus F_b, can be compressive or tensile. Although the direction of $F_{b,\min}$, (or F_b) in the concrete section would not have any effect on the behaviour of the beam, because it will be equated by a force of equal magnitude acting at the same point but in the opposite direction from the steel section, the present procedure requires the direction obtained from Eq. (4.21) to be maintained. To note, the direction of $F_{b,\min}$ is also the direction of F_b.

4.9.2. Location of PNA for partial shear connection

In determining the plastic moment capacity of a composite beam with partial shear connection, the locations of the plastic neutral axis (PNA) must be determined first. The determination requires knowledge of the magnitude and direction of F_b, for which a method has been outlined in Section 4.9.1. Once these are known, the next step is to identify the strip in which the PNA is located. For longitudinal equilibrium in the concrete section, the PNA lies in strip p_c when:

$$\sum_{s=S-k+1}^{S} \left(P_{e\leq f/g,c}\right)_s + F_b > \sum_{s=1}^{S-k} \left(P_{g,t}\right)_s \quad (4.22)$$

where $p_c = S - k_c + 1$ and k_c is the kth attempt in which Eq. (4.22) is satisfied. For longitudinal equilibrium in the steel section, the PNA lies in strip p_s when:

$$\sum_{s=S-k+1}^{S} \left(P_{e>f,c}\right)_s > \sum_{s=1}^{S-k} \left(P_{e>f,t}\right)_s + F_b \quad (4.23)$$

where $p_s = S - k_s + 1$ and k_s is the kth attempt in which Eq. (4.23) is satisfied.

The exact location of the PNA can then be determined as follows. The height of the PNA in the concrete section measured from the lowest *local* point of strip p_c, h_{pc}, can be obtained by solving the following equality:

$$\sum_{i=0} \left(P_{e\leq f/g,c}\right)_{p_c+i+1\leq S} + \left(\sum P_{e\leq f,c}\right)_{p_c,c} + F_b = \sum_{i=0} \left(P_{g,t}\right)_{p_c-i-1\geq 1} \quad (4.24)$$

while the equality for determining the height of the PNA in the steel section h_{ps} is given as:

$$\sum_{i=0} \left(P_{e>f,c}\right)_{p_s+i+1\leq S} + \left(\sum P_{e>f,c}\right)_{p_s,c} = \sum_{i=0} \left(P_{e>f,t}\right)_{p_s-i-1\geq 1} + \left(\sum P_{e>f,t}\right)_{p_s,t} + F_b \quad (4.25)$$

where the partial values can be determined by replacing the integration limit, y_n, with $y_n - h_{pc}$ and h_{pc} of the compressive part and the tensile part of the concrete, respectively, or $y_n - h_{ps}$ and h_{ps} of the steel part, respectively.

4.9.3. Plastic moment capacity for partial shear connection

Once h_{pc} and h_{ps} are determined, the individual section contributions to the plastic moment capacity, M_{conc} and M_{steel}, can be determined, as follows:

$$M_{\text{conc}} = \sum_{i=0} \left(P_{e\leq f/g,c} z_{e\leq f/g}\right)_{p_c+i+1\leq S} + \left(\sum P_{e\leq f,c} z_{e\leq f,c}\right)_{p_c,c} - \sum_{i=0} \left(P_{g,t} z_g\right)_{p_c-i-1\geq 1} \quad (4.26)$$

$$M_{\text{steel}} = \sum_{i=0} \left(P_{e>f,c} z_{e>f}\right)_{p_s+i+1\leq S} + \left(\sum P_{e>f,c} z_{e>f,c}\right)_{p_s,c} - \sum_{i=0} \left(P_{e>f,t} z_{e>f}\right)_{p_s-i-1\geq 1} - \left(\sum P_{e>f,t} z_{e>f,t}\right)_{p_s,t} \quad (4.27)$$

in which the zs are the lever arm of an element measured from the bottom of the cross-section. These lever arms are given in general terms as follows. To obtain the value for a particular group of elements, just add to the subscript e the relevant range, either $\leq f$ or $> f$, and add to the subscript p the relevant subscript, either c or s:

$$z_e = y_e + z_n \quad \text{or} \quad y_b + z_n \quad (4.28)$$

$$z_{e,c} = y_e + h_p + z_n \quad (4.29)$$

$$z_{e,t} = y_e + z_n \quad (4.30)$$

$$z_g = y_b + z_n. \quad (4.31)$$

Finally, the plastic moment capacity of the composite cross-section for partial shear connection, M_{partial}, is given as:

$$M_{\text{partial}} = M_{\text{conc}} + M_{\text{steel}}. \quad (4.32)$$

4.9.4. Note on the existing formulation [12]

Flexural strength formulations for a profiled composite beam of the type shown in Fig. 13(a) have been derived by Oehlers et al. [12] for both the full and the partial shear connection conditions. The formulations require the cross-section to be simplified into the equivalent form shown in Fig. 13(b). Based on this simplified cross-section, the formulations apply specifically to a cross-section consisting of a steel trough (formed by two steel webs, which are connected at the base by a steel flange) that surrounds a rectangular concrete core reinforced in tension. This limitation is apparent in the formulation for the plastic moment capacity for the partial shear connection, given as follows:

$$M_{\text{partial}} = F_{py}\overline{y} - 2t_e f_{py}(1+\beta)N_p^2 + F_b d_b + \left(F_{sy}d_e - \frac{1}{2}0.85\gamma^2 f_c w_e N_c^2 - F_b d_b\right) \quad (4.33)$$

in which:

F_{py} is the resultant force for the whole steel section $= (2D_e + w_e)t_e f_{py}$

$\overline{y}$ defines the point of action of F_{py}

D_e, t_e, w_e are simplified geometrical properties shown in Fig. 13

f_{py} is the profiled sheeting yield stress

N_p is the depth of the plastic neutral axis in the steel section measured from the upper surface of the cross-section

d_b and d_e define the points of action of F_b and F_{sy}, respectively

F_{sy} is the resultant force from the tensile reinforcement

f_c is the concrete compressive strength

N_c is the depth of the plastic neutral axis in the concrete section measured from the upper surface of the cross-section

β is a reduction factor used in considering the effect of local buckling (taken in this procedure as unity)

γ is a concrete nonlinearity correction factor (taken in this procedure as unity).

The limitation due to the required geometrical simplification is evident from the 2 multiplier, as it represents the two straight-rectangular-vertical webs of the profiled sheeting. Should the number of webs be different from two, or the steel component be irregular in shape, the formulation is no longer valid. Another limitation is also obvious, since there is no compression reinforcement term in Eq. (4.33). Such limitations are not present in the new procedure.

4.9.5. Plastic moment capacity of extreme conditions

The plastic moment capacity of the full shear connection and zero shear connection conditions can be determined by setting the value of F_b in each of Eqs. (4.22)–(4.25) equal to $F_{b\min}$ or to zero, respectively.

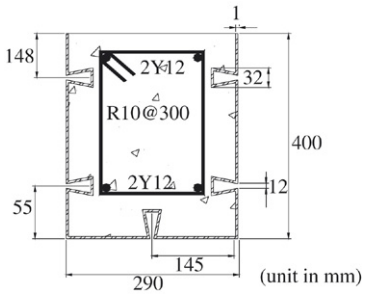

(a) Actual cross-section.

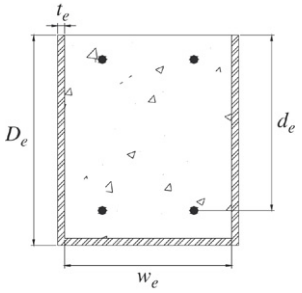

(b) Simplified cross-section.

Fig. 13. Analyzed cross-section [13,14] — (Example 3).

5. Worked examples

A program has been written using Matlab7 [8] to implement the above procedure and has been used to perform calculations for the following examples. The basic structure of the program is the conversion of the physical description of the cross-section into a series of matrix operations. This is made possible by the notation system and the discreteness of the formulation procedure. For example, the area of the eth *area element* in the sth strip is expressed by Eq. (4.1) as $(A_e)_s$. But, if element numbering and strip numbering are treated as the columns and the rows of a matrix AE, the area can equally be expressed as AE(s, e) and so become an element of matrix AE. Readers are encouraged to observe the given Matlab program scripts, which illustrate exactly how the formulations are put into practice. In particular:

(i) Terms expressed in capital letters are complete matrices, i.e. FE, TE, etc.

(ii) Terms where the first letter is a capital refer to incomplete matrices, i.e. Ae, Aef, etc. These matrices are incomplete, because they contain the components according to the specific group of elements, i.e. *area, line, bar*. They are later algebraically added to form a complete matrix.

(iii) Terms expressed in lower-case letters refer to a component of a matrix, i.e. ae, aef, etc.

5.1. Example 1

The first example deals with the properties of the single strip illustrated in Fig. 14; this is strip $s + 1$ from Fig. 7. The input data for the calculation are prescribed 'directly' in matrix form. These input data are obtained from the *physical stage*. In

Table 5.1
Summary of the prescribed matrices of Example 1

Name	Size	Section	Element	Description
FE	(S, G)	3.4	$f_{e>f}(y)$	– contains the functions that define the shape of a *line element* – the first f and the last g columns are zero vectors since only *line elements* possess function.
TE	(S, G)	3.3	$t_{e>f}$	– contains the thickness of *line element* – similar description as FE
ACTIVE	(S, G)	3.3	1 or 0	– used to distinguish between *active* and *passive* elements – set 1 for *active elements* – set 0 for *passive elements*
YN	$(S, 1)$	3.5	y_n	– defines the depth of a strip

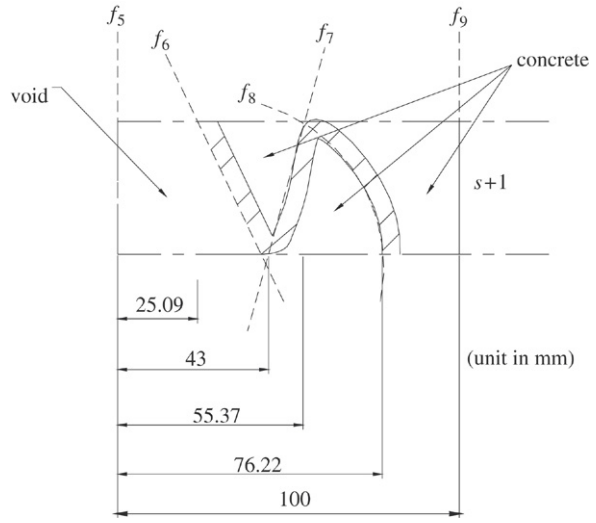

Fig. 14. Geometries of the $(s + 1)$th strip (previously shown in Fig. 7).

determining the element areas and the centroid, the following prescribed matrices are required:

(i) element function matrix, FE;
(ii) element thickness matrix, TE;
(iii) element activeness matrix, ACTIVE;
(iv) element local height vector, YN.

These prescribed matrices are given in Table 5.1. In forming the element function matrix, FE, the functions that describe the shape of the steel sheeting (f_6, f_7 and f_8) and the borders (f_5 and f_9), as shown in Fig. 14, are defined as (units in mm):

(i) $f_5 = 0$;
(ii) $f_6 = 0.49y - 43$;
(iii) $f_7 = 0.34y + 43$;
(iv) $f_8 = -0.0188y^2 + 0.1031y + 75.934$;
(v) $f_9 = 100$.

The terms f_5, f_6, f_7 and f_9 are straightforward functions; f_8 is approximated by first obtaining the coordinates of the curve at several locations using AutoCAD/2000i [1] drawing. These are plotted and used in a regression analysis written in Microsoft Office Excel 2003 [9] to generate the equation for f_8.

These functions are then assembled in the FE matrix by placing them in the $s + 1$ row. FE is an $S \times G$ matrix, where G is the highest numbered element possible in a strip within the cross-section. For strips with fewer elements, the sequential subscript numbering, as explained in Section 3.3, should be maintained. For example, for strip s of Fig. 5, the byproduct of e_3, e_4, e_8, e_9 and e_{11} of the strip should be set to zero, since it contains only two *area elements*, three *line elements*, and one *bar element* (see Box I).

Repeating the foregoing steps, the other prescribed matrices are given in Box II:

Matlab7 script (Formulations) (See Box III)

Program output

The program outputs are actually the results of the *application stage* in the form of matrices. Matrices AE and YE contain the calculated element area and centroid of the strip under consideration, given as in Box IV:

5.2. Example 2

Herein, the iteration used to determine the strip within which the PNA is located is demonstrated by the use of Eq. (4.19). The program script is given below.

Assume a cross-section discretized into five strips, as shown in Fig. 15. The assumed compressive and tensile resistances of each strip, calculated by the use of Eqs. (4.14a) and (4.14b), are shown in the figure and are assembled below as column vectors, RC and RT, respectively (units of N):

$$\mathrm{RC} = \begin{bmatrix} 255\,000 \\ 110\,000 \\ 1054\,200 \\ 345\,020 \\ 510\,000 \end{bmatrix} \quad \mathrm{RT} = \begin{bmatrix} 0 \\ 110\,000 \\ 442\,190 \\ 128\,270 \\ 0 \end{bmatrix}.$$

The iteration process for determining the location of the PNA is:

1st *attempt* $(k = 1)$

$$\sum_{S-k+1}^{S} R_c = \sum_{5-1+1=5}^{5} R_c = \mathrm{RC}(5, 1) = 510\,000$$

$$\sum_{1}^{S-k} R_t = \sum_{1}^{5-1=4} R_t = \mathrm{RT}(1, 1) + \mathrm{RT}(2, 1) + \mathrm{RT}(3, 1) + \mathrm{RT}(4, 1) = 680\,460$$

since $\sum_{S-k+1}^{S} R_c < \sum_{1}^{S-k-1} R_t$, proceed with the iteration.

$$
\mathrm{FE} = \begin{array}{c} \\ 1 \\ \\ s+1 \\ \\ S \end{array}
\begin{array}{c}
\begin{array}{cccc|cc|cc|c|cc}
1 & 2 & 3 & 4 & 5 & 6 & 7 & 8 & 9 & 10 & 11 \\
\multicolumn{4}{c}{f} & \multicolumn{2}{c}{} & \multicolumn{2}{c}{f+1} & & \multicolumn{2}{c}{g}
\end{array} \\
\left[\begin{array}{cccc|cc|cc|c|cc}
\cdot & \cdot & \cdot & \cdot & \cdot & \cdot & \cdot & \cdot & \cdot & \cdot & \cdot \\
\cdot & \cdot & \cdot & \cdot & \cdot & \cdot & \cdot & \cdot & \cdot & \cdot & \cdot \\
0 & 0 & 0 & 0 & 0 & (0.49y-43) & (0.34y+43) & (-0.0188y^2+0.1031y+75.934) & 100 & 0 & 0 \\
\cdot & \cdot & \cdot & \cdot & \cdot & \cdot & \cdot & \cdot & \cdot & \cdot & \cdot \\
\cdot & \cdot & \cdot & \cdot & \cdot & \cdot & \cdot & \cdot & \cdot & \cdot & \cdot
\end{array}\right]
\end{array}
$$

Box I.

$$
\mathrm{TE} = \begin{array}{c} \\ 1 \\ \\ s+1 \\ \\ S \end{array}
\begin{array}{c}
\begin{array}{cccc|cccc|c|cc}
1 & 2 & 3 & 4 & 5 & 6 & 7 & 8 & 9 & 10 & 11 \\
\multicolumn{4}{c}{f} & \multicolumn{4}{c}{} & f+1 & \multicolumn{2}{c}{g}
\end{array} \\
\left[\begin{array}{cccc|cccc|c|cc}
\cdot & \cdot & \cdot & \cdot & \cdot & \cdot & \cdot & \cdot & \cdot & \cdot & \cdot \\
\cdot & \cdot & \cdot & \cdot & \cdot & \cdot & \cdot & \cdot & \cdot & \cdot & \cdot \\
0 & 0 & 0 & 0 & 0 & 2 & 2 & 2 & 0 & 0 & 0 \\
\cdot & \cdot & \cdot & \cdot & \cdot & \cdot & \cdot & \cdot & \cdot & \cdot & \cdot \\
\cdot & \cdot & \cdot & \cdot & \cdot & \cdot & \cdot & \cdot & \cdot & \cdot & \cdot
\end{array}\right]
\end{array}
$$

$$
\mathrm{ACTIVE} = \begin{array}{c} \\ 1 \\ \\ s+1 \\ \\ S \end{array}
\begin{array}{c}
\begin{array}{cccc|cccc|c|cc}
1 & 2 & 3 & 4 & 5 & 6 & 7 & 8 & 9 & 10 & 11 \\
\multicolumn{4}{c}{f} & \multicolumn{4}{c}{} & f+1 & \multicolumn{2}{c}{g}
\end{array} \\
\left[\begin{array}{cccc|cccc|c|cc}
\cdot & \cdot & \cdot & \cdot & \cdot & \cdot & \cdot & \cdot & \cdot & \cdot & \cdot \\
\cdot & \cdot & \cdot & \cdot & \cdot & \cdot & \cdot & \cdot & \cdot & \cdot & \cdot \\
0 & 1 & 0 & 1 & 0 & 1 & 1 & 1 & 0 & 0 & 0 \\
\cdot & \cdot & \cdot & \cdot & \cdot & \cdot & \cdot & \cdot & \cdot & \cdot & \cdot \\
\cdot & \cdot & \cdot & \cdot & \cdot & \cdot & \cdot & \cdot & \cdot & \cdot & \cdot
\end{array}\right]
\end{array}
$$

$$
\mathrm{YN} = \begin{array}{c} \\ 1 \\ \\ s+1 \\ \\ S \end{array}
\left[\begin{array}{c}
\cdot \\ \cdot \\ 36.69 \\ \cdot \\ \cdot
\end{array}\right]
$$

Box II.

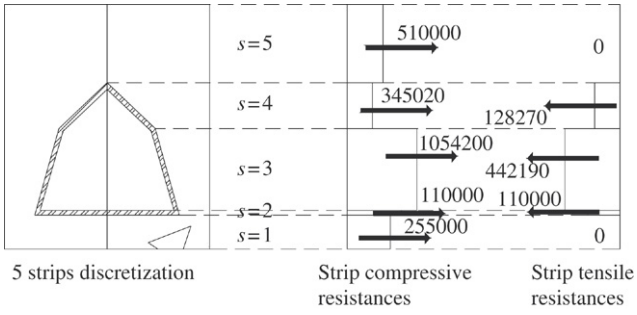

Fig. 15. Assumed cross-section resultants (units in N).

2nd *attempt* ($k = 2$)

$$\sum_{S-k+1}^{S} R_c = \sum_{5-2+1=4}^{5} R_c = \mathrm{RC}(4,1) + \mathrm{RC}(5,1) = 855\,020$$

$$\sum_{1}^{S-k} R_t = \sum_{1}^{5-2=3} R_t = \mathrm{RT}(1,1) + \mathrm{RT}(2,1) + \mathrm{RT}(3,1) = 570\,460$$

since $\sum_{S-k+1}^{S} R_c > \sum_{1}^{S-k-1} R_t$, stop iteration. $k_h = 2$ hence $p = S - k_h + 1 = 4$ (PNA lies in strip 4).

Matlab7 script

```
for k=1:S
    k
    RIGHT=double(sum(RC(S-k+1:S,1)))
    LEFT=double(sum(RT(1:S-k,1)))
    if RIGHT>LEFT
       break
     end
end
    p=S-k+1
```

5.3. Example 3 (validation of the procedure)

Application to an actual beam cross-section is demonstrated and validated by analyzing the profiled composite beam cross-section shown in Fig. 1(j). Results are then compared with those obtained from the original formulation [12]. This formulation did not allow for the actual shape of the cross-section and required the cross-section be simplified. Compression reinforcement was not included. The cross-section is the one previously studied by Uy and Bradford [13,14] shown in Fig. 13. Full shear connection is considered (the values of $F_{b\,\min}$ are as calculated in Example 5 for a partial shear connection analysis). It is also assumed that the concrete

Element area

The following is the program script for the determination of the element area written in Matlab7.

```
    Ae=zeros(S,G)
    Aef=zeros(S,G)
    Ag=zeros(S,G)
for e=1:f
for s=1:S
    ae=(int(FE(s,e+f+1)-(FE(s,e+f)+TE(s,e+f)),0,YN(s,1))) % - - - - - - - - - Equation (4.1)
    Ae=[zeros(s-1,G);zeros(1,e-1),ae,zeros(1,G-e); zeros(S-s,G)]+Ae
end
end
for e=f+1:2*f+1
for s=1:S
    aef=(int((1+(diff(FE(s,e))2̂))0̂.5,0,YN(s,1)))*TE(s,e)% - - - - - - - - - - - - - - - - - - - - Equation (4.2)
    Aef=[zeros(s-1,G);zeros(1,e-1),aef,zeros(1,G-e);zeros(S-s,G)]+Aef
end
end
for e=2*f+2:G
for s=1:S
    ag=pi*(RE(s,(e))) 2% - - - - - - - - - - - - - - - - - - - - - - - - - - - - - - - - - - - - - - - - - - - - - - - - -Equation (4.3)
    Ag=[zeros(s-1,G);zeros(1,e-1),ag,zeros(1,G-e);zeros(S-s,G)]+Ag
end
end
AE=Ae+Aef+Ag
```

Effective area

AE contains the areas of all elements including the *passive elements*. To remove these, AE is multiplied, element-by-element (using operator (.*)) by the ACTIVE matrix, as follows:

```
AE=ACTIVE.*AE
```

Element centroid

The script for the determination of the element centroid is given below.

```
    Ye=zeros(S,G)
    Yef=zeros(S,G)
    Yg=zeros(S,G)
for e=1:f
for s=1:S
       ye=((int(FE(s,e+f+1)*y-(FE(s,e+f)+TE(s,e+f))*y,0,YN(s,1)))/AE(s,e)) % - - - - - - - - - Equation (4.4)
    Ye=[zeros(s-1,G);zeros(1,e-1),ye,zeros(1,(G)-e);zeros(S-s,G)]+Ye
end
end
for e=f+1:2*f+1
for s=1:S
       yef=YN(s,1)/2% - - - - - - - - - - - - - - - - - - - - - Equation (4.5)
    Yef=[zeros(s-1,G);zeros(1,(e)-1),yef,zeros(1,(G)-(e));zeros(S-s,G)]+Yef
end
end
for e=2*f+2:G
for s=1:S
       yg=YB(s,1) % - - - - - - - - - - - - - - - - - - - - - - - - - - - - - - - - - - - - - - - - - - - - - - - - - - - - - - - - - - - - - - - - - - - - - - - - - - - - - - - - - - - - - - -Equation (4.5)
    Yg=[zeros(s-1,G);zeros(1,e-1),yg,zeros(1,G-e);zeros(S-s,G)]+Yg
end
end
YE=Ye+Yef+Yg
```

Omitting NaN and inf elements

Since AE contains zero elements, YE obtained above contains NaN (not-a-number) and/or inf (infinity) elements; terms used by Matlab7. The former occurs when zero is divided by zero, whilst the latter occurs when a number is divided by zero. To omit these elements from YE, the following script is written for the program.

```
for e=1:G
for s=1:S
if YE(s,e)== NaN
       YE(s,e)=0
else
if YE(s,e)== Inf
       YE(s,e)=0
end
end
end
end
```

Box III.

$$\mathrm{AE} = \begin{bmatrix} \cdot & \cdot & \cdot & \cdot & \cdot & \cdot & \cdot & \cdot & \cdot & \cdot & \cdot \\ \cdot & \cdot & \cdot & \cdot & \cdot & \cdot & \cdot & \cdot & \cdot & \cdot & \cdot \\ 0 & 2.981\text{e}3 & 0 & 1.0497\text{e}3 & 0 & 81.7 & 77.5 & 88.8 & 0 & 0 & 0 \\ \cdot & \cdot & \cdot & \cdot & \cdot & \cdot & \cdot & \cdot & \cdot & \cdot & \cdot \\ \cdot & \cdot & \cdot & \cdot & \cdot & \cdot & \cdot & \cdot & \cdot & \cdot & \cdot \end{bmatrix}_{s+1}$$

$$\mathrm{YE} = \begin{bmatrix} \cdot & \cdot & \cdot & \cdot & \cdot & \cdot & \cdot & \cdot & \cdot & \cdot & \cdot \\ \cdot & \cdot & \cdot & \cdot & \cdot & \cdot & \cdot & \cdot & \cdot & \cdot & \cdot \\ 0 & 18.1379 & 0 & 20.6453 & 18.3450 & 18.3450 & 18.3450 & 18.3450 & 0 & 0 & 0 \\ \cdot & \cdot & \cdot & \cdot & \cdot & \cdot & \cdot & \cdot & \cdot & \cdot & \cdot \\ \cdot & \cdot & \cdot & \cdot & \cdot & \cdot & \cdot & \cdot & \cdot & \cdot & \cdot \end{bmatrix}_{s+1}$$

Box IV.

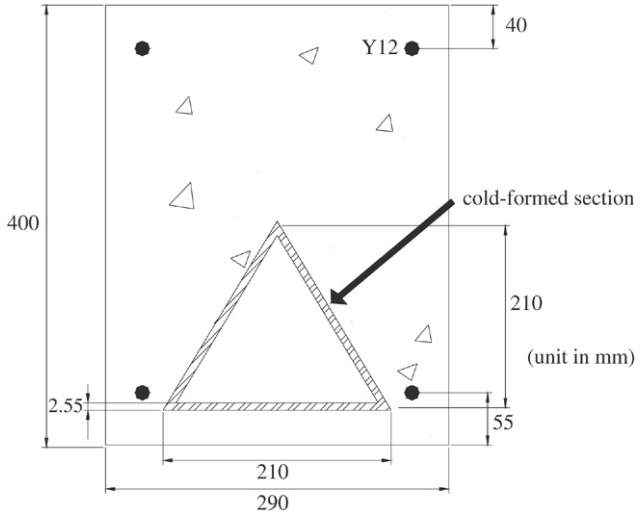

Fig. 16. PCFC beam cross-section (Example 4).

Table 5.2
Material properties (units are in N and mm) (Example 3)

Properties	Concrete	Steel sheeting	Reinforcement bar
Modulus of elasticity, E	33 100	205 000	200 000
Cylinder compressive strength, $0.85f_c$	36.89	–	–
Yield strength, p_y or $0.87f_y$	–	552	378.45

crushes throughout its compressive depth and that the steel does not buckle locally. For the simplified cross-section, the compressive reinforcements are ignored. The geometrical and material properties of the cross-section are given in Table 5.2.

Geometry of the simplified cross-section (units in mm):

$$t_e = 1.63 \quad D_e = 388.76 \quad d_e = 345 \quad w_e = 283.4.$$

For validation, a direct comparison is made between the proposed procedure and the original formulation by first determining the plastic moment capacity of the simplified cross-section. To demonstrate the advantages of the proposed procedure, the cross-section is then analyzed for its actual shape. The results of the analyses are given in Table 5.3.

Table 5.3
Calculated plastic moment capacities (Example 3)

Formulation	Plastic moment capacity (N mm)	
	Actual shape	Simplified shape
Existing [12]	–	2.2595×10^8
Proposed	2.3851×10^8	2.2595×10^8

Comparison between the results of both methods for the simplified shape validates the proposed procedure. It can also be observed that the use of the simplified shape yields a conservative result (5.6% lower). This is partially due to the fact that the compression bars were not included in the calculation. Including these (only possible using the proposed procedure), but still working with the simplified shape increases the resistance to 2.286×10^8 N mm (4% discrepancy); the remaining difference is thus the result of the simplification of the actual shape.

5.4. Example 4 (PCFC beam)

The efficiency of the proposed PCFC cross-section in terms of second moment of area and plastic moment capacity is demonstrated by comparing its capacities with the profiled composite beam analyzed previously. The PCFC beam has the same width, height, material properties and amount of steel as the profiled composite beam. The geometrical properties of the PCFC beam are shown in Fig. 16. The simple shape of the cold-formed section is provided for readers who are interested to verify the calculation.

The results of the analyses are tabulated in Table 5.4. Based on these, it is found that, for the same amount of steel, the PCFC beam possesses a higher plastic moment capacity by about 7% for a reduction in concrete volume of about 23.5%. The increase in strength is due to the former section having greater eccentricity of force resultants compared to the latter. However, this improvement in the ultimate performance of the beam is accompanied by a reduction in the second moment of area. As tabulated, the uncracked second moment of area of the PCFC beam is 14.6% lower than that of the profiled composite beam. This reduction is due to the hollowness of the PCFC beam. The reduction is even greater for the cracked second moment of

Table 5.4
Calculated flexural properties of the beams (Example 4)

Beam	ENA height (mm)	PNA height (mm)	Second moment of area (mm^4)		Plastic moment capacity (N mm)
			Uncracked	Cracked	
Uy and Bradford [13]	204.4843	326.2980	2.6348×10^8	1.4927×10^8	2.3851×10^8
PCFC	220.7515	310.5771	2.2984×10^8	1.1784×10^8	2.5627×10^8

Note: ENA and PNA heights are measured from the bottom of cross-section.

Table 5.5
Results of analysis (Example 5)

Method	$F_{b\,\min}$ (N)			Simplified shape M_{partial} of profiled beam (N mm)	Actual shape M_{partial} (N mm)	
	Direction	Actual shape	Simplified		Profiled beam	PCFC
Existing	Tensile	–	6.882×10^5	2.1064×10^8	–	–
Proposed	Tensile	-7.9366×10^5	-6.8820×10^5	2.1044×10^8	2.1369×10^8	1.8573×10^8

area, where a reduction of about 27% is calculated. The greater reduction is due to the fact that the height of the ENA in the profiled composite beam is lower than for the PCFC beam. Since the cracked second moment of area is calculated based on the assumption that concrete cracks up to the ENA, PCFC contains more cracked concrete than the profiled composite beam.

The above discussion highlights the efficiency of PCFC beams in the ultimate condition, compared to the profiled composite beam, although the former appears to be less efficient at the serviceability condition. However, it is necessary to recall all the advantages that a PCFC beam can offer as outlined previously. For example, from the cold-formed steel point of view, notwithstanding the increase in the strength due to the composite action and the solution of the stability and bearing problem due to the load introduction, the increase in the second moment of area of the PCFC beam is 77% compared to the cold-formed section acting alone. By changing the shapes, a better balance between serviceability and ultimate capacities is possible.

5.5. Example 5 (Partial shear connection)

The profiled composite beam from Example 3 is re-analyzed for the partial shear connection condition. The analysis is initiated by first determining the minimum magnitude of F_b for full shear connection, denoted $F_{b,\min}$. Once this has been obtained, a lower magnitude can be specified for the partial connection analysis of the beam. $F_{b,\min}$ is determined using both the existing method [12] and the proposed procedure, so that a check can be made. The results are compared in Table 5.5; the values of $F_{b,\min}$ and M_{partial} of the simplified shape are identical, hence the validation of the present procedure. The existing method is not able to analyze the beam based on its actual shape, hence the missing value in the appropriate box. Repeating the analysis, $F_{b,\min}$ for the PCFC beam is found to be -9.5666×10^5 N. Details of the PCFC beam are given in Example 4. Based on the results, F_b with a magnitude and a direction of -4×10^5 N is chosen as an input for the calculation of M_{partial} for both beams using the proposed procedure, and the results are given in Table 5.5. The value selected for F_b is less than the full steel axial resistance, F_s, which is calculated to be more than 950 kN. M_{partial} of the PCFC beam is about 15% lower than M_{partial} of the profiled composite beam. However, the former uses 23.5% less concrete, with the provision of only 40% shear connection (calculated as $F_b/F_{b,\min} \times 100$) as compared to the 50% in the latter.

6. Conclusions

A procedure has been presented for the calculation of the key cross-sectional properties of steel–concrete composite beams having complex cross-sectional forms. The procedure is general in terms of the shape of the cross-section. It is specifically derived in a format suitable for simple computer programming. The key feature of the procedure is the use of functions to describe the shape of each element within the cross-section, leading to the determination of the various cross-sectional properties through appropriate integrations. Motivation for the development came from the need to deal with a new type of composite beam known as the PCFC beam. This consists of a closed cold-formed steel section encased in reinforced concrete. The beam has been shown to perform better than the equivalent, more conventional profiled composite beam at the ultimate condition, although it is slightly less efficient when considering some serviceability aspects.

Acknowledgements

The first author would like to thank his sponsors, the Public Service Department of Malaysia and Universiti Teknologi Malaysia, for their financial support in his Ph.D. studies at Imperial College London. The authors would also like to thank Dr. Vellasco, Mr. Soleiman Fallah and Mr. Mohamed Ali for helpful technical discussions during the preparation of the papers.

References

[1] AutoCad LT® 2002, Copyright Autodesk, Inc.

[2] Barnard PR, Johnson RP. Ultimate strength of composite beam. Proceedings of the Institution of Civil Engineers 1965;32:101–79.

[3] Chapman JC, Balakrishnan S. Experiments on composite beams. The Structural Engineer 1964;42(11):369–83.

[4] Grant JA, Fisher JW, Slutter RG. Composite beams with formed steel deck. American Institute of Steel Construction Engineering Journal 1977; 14(1):24–42. [First quarter].

[5] Hicks S, Lawson RM, Lam D. Design consideration for composite beams using pre-cast concrete slabs, composite construction in steel and concrete V. Berg-en-Dal (Mpumalanga, South Africa): United Engineering Foundation, The Krueger National Park Conference Centre; 2004.

[6] Lam D, Elliot KS, Nethercot DA. Experiments on composite steel beams with precast concrete hollow core floor slabs. In: Proceedings of the Institution of Civil Engineers (Structures and Buildings). May 2000, 140, p. 127–38.

[7] Lange J. Design of edge beams in slim floors using pre-cast hollow core slabs, composite construction in steel and concrete V. Berg-en-Dal (Mpumalanga, South Africa): United Engineering Foundation, The Krueger National Park Conference Centre; 2004.

[8] Matlab7, Version 7.0.0 19920 9 (R14), 2004, Copyright The MathWorks, Inc.

[9] Microsoft Office Excel 2003®, Microsoft Corporation.

[10] Nethercot DA, editor. Composite construction. Spon Press; 2003.

[11] Oehlers DJ. Composite profiled beams. Journal of Structural Engineering, ASCE 1993;119(4):1085–100.

[12] Oehlers DJ, Wright HD, Burnet MJ. Flexural strength of profiled composite beams. Journal of Structural Engineering, ASCE 1994;120(2): 378–90.

[13] Uy B, Bradford MA. Ductility and member behaviour of profiled composite beams: Experimental study. Journal of Structural Engineering, ASCE 1994;121(5):876–82.

[14] Uy B, Bradford MA. Ductility and member behaviour of profiled composite beams: Analytical study. Journal of Structural Engineering, ASCE 1994;121(5):883–9.